*Proceedings of the*
*Annual Stability Conference*
*Structural Stability Research Council*
*San Antonio, Texas, March 21-24, 2017*

# Nonlinear Behavior of Global Lateral Buckling of I-Girder Systems

Liwei Han[1], Todd Helwig[2]

## Abstract

I-girder systems with relatively long spans and narrow widths are susceptible to a system buckling failure mode that is relatively insensitive to the spacing between cross frame or diaphragm braces. This global buckling mode is of particular concern during deck placement and can compromise the safety and/or constructability of steel bridge systems. This paper presents computational studies on the nonlinear behavior of a variety of steel I-girder systems. A number of geometric factors affecting the nonlinear buckling behavior of I-girder systems such as the shape and distribution of the imperfection along the length as well as the girder curvature were investigated. The process of cross frame installation was simulated to investigate the impact of the installation process of the braces on the resulting behavior. The results demonstrate that the susceptibility of the system mode of buckling to 2nd order amplification is significantly reduced compared to the "critical-shape imperfection". The initial girder imperfection was significantly altered by fit-up of cross frames and the likely imperfection pattern afterwards. The FEA results demonstrate that the "critical shape" imperfection that has been used for stability bracing of cross frame systems may not be likely to occur in practice. The results of this study provide insight into adequate limits on second-order displacement amplification of I-girder systems under transverse non-composite loading.

## 1. Introduction

I-Girder systems that have relatively long spans and a narrow width are susceptible to a failure mode involving the lateral-torsional movement of the girder system as a structural unit. The failure mode is referred to as either global lateral buckling or system buckling and is analogous to the lateral-torsional buckling mode (LTB) of individual girders which occurs between the intermediate bracing. However, the system mode of buckling of the girder system has a buckling mode shape usually consisting of a half-sine curve along the span length between the bridge supports and is relatively insensitive to the spacing between intermediate cross frames or diaphragms.

The critical stage for the system mode of buckling usually occurs during the deck placement where the steel girder system must support the entire loading before the concrete deck has cured. Although historically not considered by design specifications, this mode of structural failure has

[1] Former Graduate Research Assistant, The University of Texas at Austin, <hanliwei@utexas.edu>
[2] Professor, The University of Texas at Austin, < thelwig@mail.utexas.edu>

increasingly drawn attention due to bridge failures over recent decades such as the collapse of the Marcy Pedestrian Bridge during concrete deck placement (Yura and Widianto 2005). Yura et al. (2008) outlined the results of analytical and numerical studies of simply-supported twin I-girder systems and developed a simplified expression for the elastic global buckling resistance of the simply-supported twin I-girder system under non-composite loading:

$$M_g = \frac{\pi^2 sE}{L^2}\sqrt{I_y I_x} \tag{1}$$

This expression reveals that the resistance of the girder systems to the global lateral buckling primarily results from the warping stiffness of the girder system. The moment resistance $M_g$ calculated by Eq. (1) represents the total capacity of the girder system and should be compared with the sum of the maximum girder moments across the width of the system. As with many global instabilities, the system buckling mode does not occur in a sudden manner as described by a mathematical bifurcation, but rather, is usually preceded by excessive second-order amplification of lateral-torsional displacements. A number of closely-spaced 2- and 3-girder systems have experienced problems during deck pours, severely compromising the safety and constructability of bridge systems. Nevertheless, the elastic critical buckling load given by Eq. (1) serves as a theoretical upper limit and an important indicator of the structural susceptibility to the second order global displacement amplification (Sanchez and White 2012). The AASHTO specifications (2015) included Eq. (1), along with a 50% limitation for the sum of the moments to mitigate excessive second order amplifications.

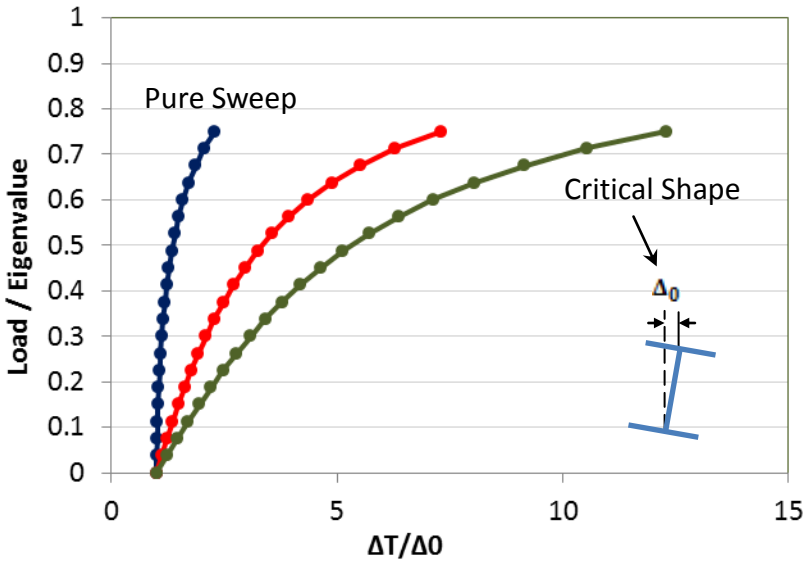


Figure 1. Force vs Lateral Displacement Curves for Different Shapes (Han and Helwig 2016)

In an earlier study (Han and Helwig 2016), parametric finite element analyses were performed extending the study of the elastic global buckling capacity from simply-supported I-girder systems to continuous I-girder systems. Nonlinear buckling analyses were carried out to investigate the impact of the cross-sectional shape of imperfection on the susceptibility of an imperfect simply-supported twin I-girder system to the second-order displacement amplification as shown in Fig.1. The "critical-shape" of the imperfection was the same as reported in Wang

and Helwig (2005) and consists of a straight bottom flange with a lateral sweep of the top flange. However, in recent studies, the likelihood of such an imperfection to occur in practice is somewhat questionable. Although this imperfection is a viable shape of the steel girder without intermediate braces, cross frames are fabricated with a very specific geometry. The erectors depend on the cross frames to help control the geometry and often must pull the girders into place using chains or drift pins as the cross frames are fit into place. Obviously, the cross frames will play an important role in the final geometry of the erected steel girder system and it is therefore important to consider this final geometry when evaluating the girder behavior from the perspective of the system buckling mode during placement of the concrete bridge deck. Therefore, the likely girder imperfection pattern after cross-frame installation needs further study, which is one of the goals of the study outlined in this paper.

In addition, although Eq. (1) provides a good solution for prismatic, doubly-symmetric girder systems that are simply supported, most steel girder systems have greater geometric complexities. Many girder systems are non-prismatic and are continuous over multiple supports. In addition, some of the girders have mild degrees of horizontal curvature, which will significantly affect the behavior of the system. Therefore, an in-depth study of the nonlinear buckling behavior of such systems is prudent. This paper outlines computational studies consisting of:

1) A simulation of the cross frame installation process for girder systems with a variety of initial imperfection distributions to provide insight into how the initial girder imperfection is altered by the fit-up of cross frames and the likely imperfection distribution of the fully erected steel girder system;
2) Investigations of the geometric factors that affect the nonlinear buckling behavior of I-girder systems such as cross-sectional shape of imperfection, distribution of imperfection along the length, and girder curvature; and,
3) Developing proper limits on second-order displacement amplification of I-girder systems as a function of the geometry of the system.

## 2. Finite Element Model

Three-dimensional FE Analyses were performed utilizing ANSYS Ver. 14.5 (2015) for this study to investigate the non-linear buckling behavior of narrow I-girder systems. The material model of the steel was assumed linear elastic, with the Young's Modulus $E$ = 29,000 ksi and Poisson's ratio $\nu$ = 0.3.

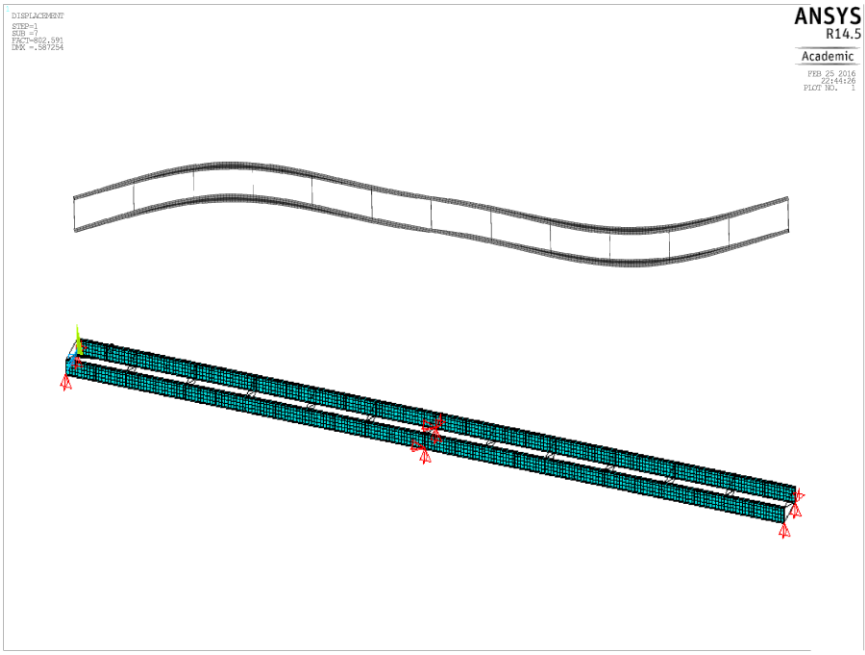


Figure 2. FE Model of a Two-span Twin I-girder System and Buckled Shape

The steel girders were modelled using 8-node shell elements (SHELL281) for the flange and web plates as well as transverse stiffeners. The shell elements possess three translational and three rotational degrees of freedom at each node. This element has quadratic displacement shape functions, which are suited to model either straight or horizontally-curved girder geometries. A finite-element model of a two-span continuous I-girder system and the buckled shape in the system mode is depicted in Fig. 2.

A standard prismatic cross section was used for all analyses as illustrated in Fig. 3(a). It is comprised by two 14 in. × 1.5 in. flanges and a 56 in. × 0.625 in. web plate, resulting in a flange-to-depth ratio of ¼, which is representative of the geometries often used in bridge design practice (Stith 2010). As shown in Fig. 3(b), each flange was modeled with an element on either side of the web and four elements through the depth of the web plate.

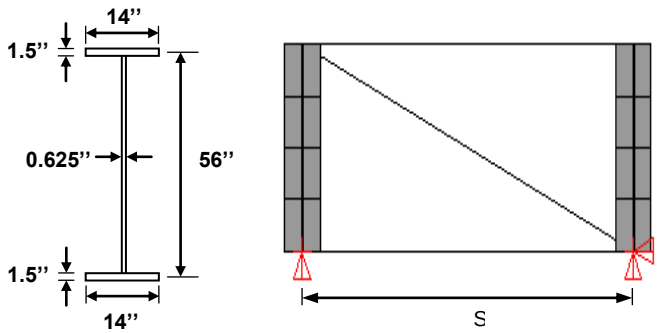


Figure 3. (a) Standard Cross Section (b) Tension-only Cross Frame

Despite the fact that most cross frame types consist of either X-type (2 diagonals) or K-type cross frames, the single diagonal "tension-only" Z-type cross frame was used for the finite-element model, as shown illustrated in Fig. 3(b). This cross frame was selected for simplicity and the layout of the cross-frame does not have any impact on the global buckling mode. Although a recent research study (Battistini et al. 2016) indicates the stiffness reduction caused by the eccentric connection of the single angles, it is not necessary for this model since truss elements with no eccentricity were used in the model. The cross frame was modeled using the properties of L4×4×1/2 steel angles with a sectional area of 3.75 $in^2$. The spacing between the cross frames was 20 ft. for all analyses. This cross frame configuration ensures that the individual girders were adequately braced in the trial elastic analyses. The steel angles that comprise the cross frames were modeled using the 3D space truss element LINK180. The braces share the coincident nodes with shell element at the girder and cross frame interfaces. The girder cross sections were free to warp at the supports. These assumptions are consistent with previous research studies of steel girder buckling (Helwig 1994; Quadrato 2010; Battistini et al. 2016).

**3. Cross-frame Installation Simulation**

The previous study (Han and Helwig 2016) that investigated the critical shape of imperfection of a simply-supported twin girder system found the worst-case to occur when the bottom flange is perfectly straight and the top flange has a lateral sweep of L/1000, where L is the span length. This shape is consistent with the findings of Wang and Helwig (2005) that studied the critical shape imperfection for torsional bracing provided by cross frames. However, this critical shape assumes that the cross frames will "fit" into the structure allowing the bottom flange to stay straight while the top flange has a lateral sweep. In reality, cross frames are fabricated with a very controlled geometry in which the two diagonals are essentially the same length, as are the top struts. In general, the only discrepancy in the cross frame geometry from the desired geometry are the "girder drops" which represent the desired girder cambers as well as other limitations the specific bridge geometry that may occur during erection (bridge support skew, horizontal curvature, etc.). As a result, although the girders will possess a specific imperfection within common fabrication tolerances, the cross frame geometry will often be very close to a "perfect fit". The erector will actually depend on the cross frames to assist in maintaining the bridge geometry.

One of the goals of the study discussed in this paper was to determine the behavior of the girders as cross frames are installed into an imperfect girder system. The cross frames were then built to fit the imperfect girders geometrically to maintain the critical cross-sectional shape of imperfection. Because cross frames are usually fabricated in a rectangular shape in practice and their ability to resist in-plane distortion is typically far greater than the torsional rigidity of a girder, the resulting geometry will likely be much different than the "critical shape". During cross frame installation, the girders will usually be forced into place using a combination of chains, drift pins, and other erection equipment. A simulation of the cross frames installation process for a simply-supported twin I-girder system during the process of girder system erection was carried out to investigate the impact of cross frame fit-up on the initial girder imperfections and the likely cross-sectional shape of imperfection after the installation.

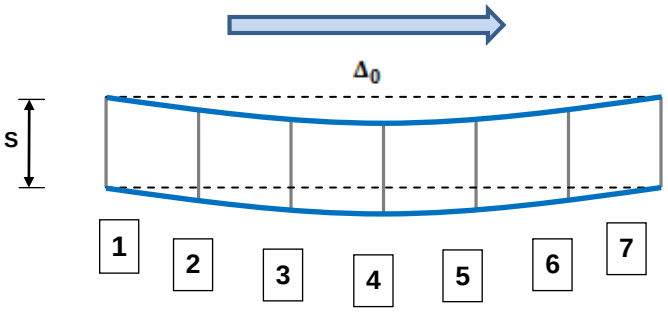

Figure 4. Plan View of Twin I-girder Sequence of Cross Frame Fit-up

As depicted in Fig. 4, a load-deflection analysis was performed on a simply-supported twin girder system that spanned 120 ft. with a girder spacing of 7 ft. It has a standard girder section and a single wave imperfection distribution along the length with a maximum value $\Delta_0 = L/1000 = 1.44$ in. at mid-span.

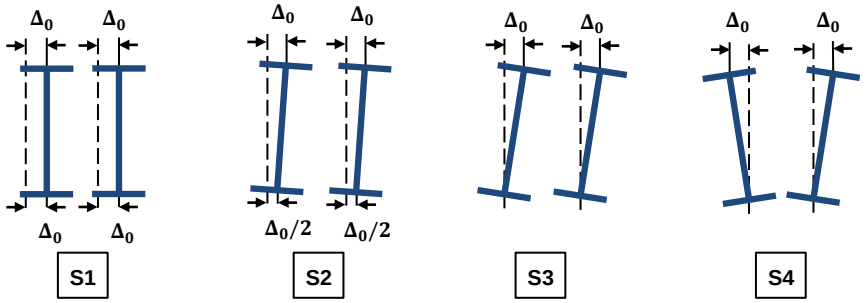

Figure 5. Different Cross-sectional Shapes Considered

As illustrated in Fig. 5, four cross-sectional shapes labeled S1-S4, which include S1 - "pure sweep", S2 - "Partial Critical Shape", S3 - "Critical-Shape", and S4 - "Asymmetric Critical Shape" types, were considered in the analyses. The simulation of the cross frame installation process was modeled in 4 steps as illustrated in Fig. 6.

Step 1: The twin girders with geometric imperfections were built and two end cross frames (Number 1 and 7) were attached in the girders directly because the imperfection is zero at the supports.
Step 2: The two girders were pulled straight by applying displacement loads at the location where a cross frame was to be installed.
Step 3: The cross frame was attached to the girders with the "perfect" geometry established in Step 2.
Step 4: The previously-applied displacement restraints were removed at this location after the cross frame fit-up and thereby the girder is released. The girder system was then allowed to displace to the position of equilibrium between the "imperfect girder" and "perfect cross frame".

Steps 2 through 4 were then repeated for each subsequent cross frame until the full erection process was simulated.

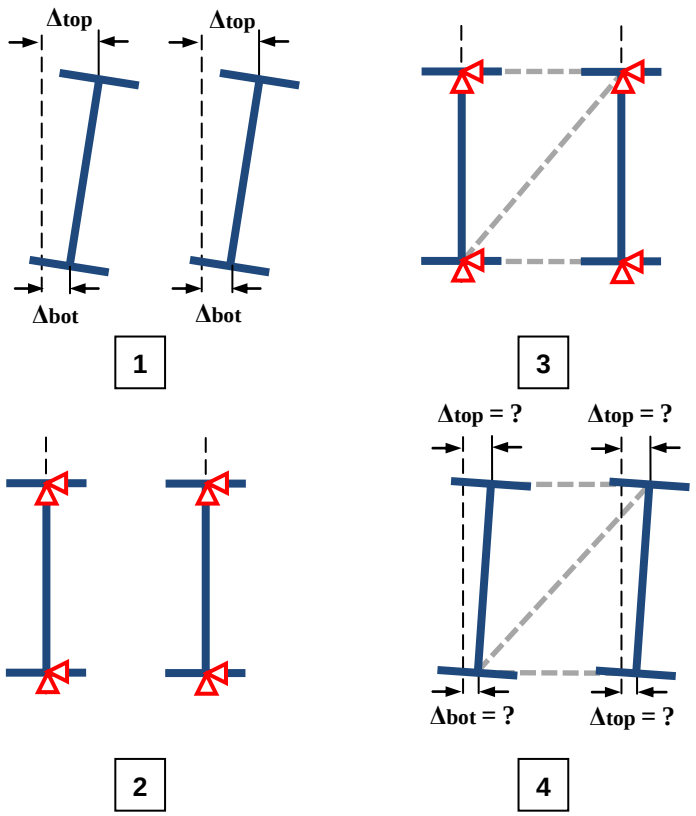

Figure 6. Load Steps of Cross Frame Fit-up Simulation

For the analysis discussed in this example, the cross-frame fit-up process progressed for cross frames 2 to 6 (Figure 4). The parameters for cross-sectional shapes of imperfection at mid-span after the installation were compared with the initial values as provided in**Error! Reference source not found.** Table 1. It is evident that lateral displacement values for top and bottom flanges of both girders had converged after the cross frame installation for all four cross-sectional shapes. A reasonable explanation would assume that the cross-sectional imperfection of an individual girder might be decomposed into a lateral and a rotational component. The cross frame fit-up tended to diminish the rotational components at each location while the lateral components of the two girders approach to a median value due to displacement compatibility. Focusing on Shape S3, which has been identified as the "critical shape" that tends to result in the largest second order amplification, the initial and final imperfection before and after the installation of the cross frames are markedly different. The initial imperfection prior to installation of the cross frames had a lateral sweep of 1.44" (L/1000) at the top flange with a straight bottom flange. After installation of all of the cross frames both flanges had nearly the same lateral sweep with a value near L/2000 which is 0.72". The resulting imperfection is very close to a "pure sweep". As a result, the critical shape imperfection for the system buckling mode should more likely be the case of a "pure sweep" of L/1000, which is the S1 imperfection. As a result, in the remainder of this paper, only the "pure sweep" type cross-sectional shape S1 is considered for the non-linear analyses, since the three other imperfection shapes produced smaller imperfections in the fully erected girder system.

Table 1. Girder flange displacements before and after the cross frame installation

| | | S1 | | S2 | | S3 | | S4 | |
|---|---|---|---|---|---|---|---|---|---|
| | | $\Delta_{top}$ (in.) | $\Delta_{bot}$ (in.) | $\Delta_{top}$ (in.) | $\Delta_{bot}$ (in.) | $\Delta_{top}$ (in.) | $\Delta_{bot}$ (in.) | $\Delta_{top}$ (in.) | $\Delta_{bot}$ (in.) |
| Girder 1 | Before | 1.44 | 1.44 | 1.44 | 0.72 | 1.44 | 0.00 | -1.44 | 0.00 |
| | After | 1.44 | 1.44 | 1.10 | 1.06 | 0.75 | 0.69 | 0.00 | 0.00 |
| Girder 2 | Before | 1.44 | 1.44 | 1.44 | 0.72 | 1.44 | 0.00 | 1.44 | 0.00 |
| | After | 1.44 | 1.44 | 1.10 | 1.06 | 0.75 | 0.69 | 0.00 | 0.00 |

Note: $\Delta_{top}$ = Lateral displacement of top flange; $\Delta_{bot}$ = Lateral displacement of bottom flange

## 4. Critical distribution of imperfection

The non-linear buckling analyses discussed so far have focused on the behavior of simply-supported systems. For continuous systems with two spans or more, the girder imperfection within one span also will likely affect the nonlinear bucking behavior of the neighboring spans. The critical distribution of imperfection for continuous systems that leads to the largest second-order lateral-torsional displacement requires further understanding.

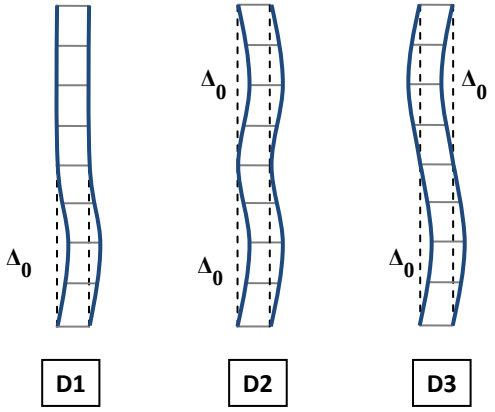


Figure 7. Distributions of Imperfection Considered

To investigate this effect, nonlinear load-deflection analyses were performed on a two span continuous twin I-girder system equally spanned by 140 ft. and spaced 7 ft. apart with standard girder section. Given the findings from the previous section, a "pure sweep" shape imperfection was assigned to both girders with a single wave distribution and a maximum value $\Delta_0 = L/1000 =$ 1.68 in. at mid-span consistent for any individual spans where girder imperfections are considered. As depicted in Fig. 7, three cases labeled D1 to D3 that account for different combinations of imperfection distributions with varying lateral directions in each span were analyzed.

For Case D1, the imperfections were only imposed on one span while the other span keeps straight. For Case D2, girder imperfections were applied to both spans with same lateral direction, whereas the lateral direction of girder imperfection alternated in two spans for Case D3, forming a zigzagging distribution pattern along the length.

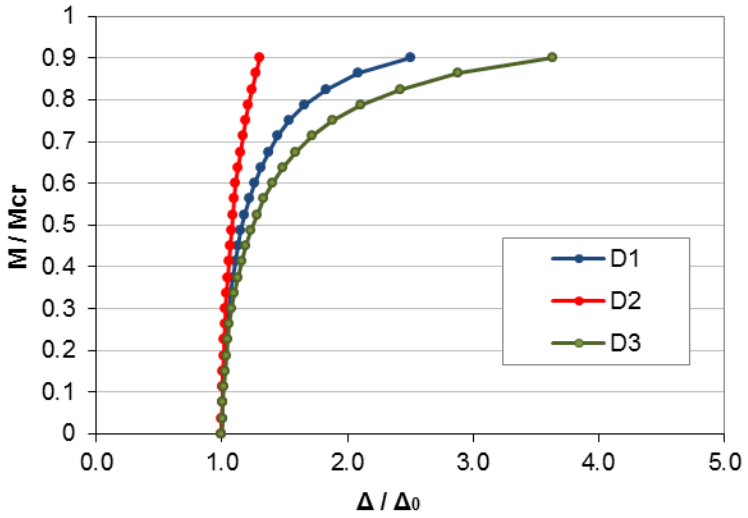


Figure 8. Effect of Distribution of Imperfection on Displacement Amplification

Fig. 8 presents a curve of normalized load versus maximum lateral displacement which is examined at mid-span for all three cases. The loads are normalized by the elastic buckling loads while the lateral displacement is normalized by the maximum initial imperfection $\Delta_0$. It can be observed that the most critical shape is Case D3 in which the lateral directions of imperfection distribution alternated among neighboring spans forming a zigzagging pattern. The reason for this critical imperfection distribution can be explained by the resemblance to the buckled shape of the continuous girder system as depicted in Fig. 2. This is consistent with many studies on instabilities in which eigenvalue buckling solutions are used for "seed" imperfections. At 70% of the elastic buckling loads, the normalized lateral displacement for the critical Case D3 is only 0.67 (1.13 in.).

$$M_g = C_{bs} \frac{\pi^2 sE}{L^2} \sqrt{I_y I_x} \tag{2}$$

As a result of the previous study and this study, the AASHTO (2015) limitation to 50% of the critical load (Eq.(1)) appears overly-conservative. A twofold moment gradient value $C_{bs}$ is proposed in addition to Eq. (1). The constant value of 1.1 for simply-supported systems and 2.0 for continuous girder systems are recommended. The sum of girder moment across the width is limited to 70% of the Eq. (2) to avoid excessive second-order amplification.

## 5. Curved girder systems

Given the results from the previous analyses, the initial girder imperfection distribution pattern has a profound impact on the nonlinear buckling behavior of the I-girder system. Concerns have been consequently raised over curved girder systems, whose curved geometries are of similar character to the straight girder systems with single wave imperfection distributions. Although curved girder systems do not tend to experience "bifurcations" many engineers still use the buckling solutions as an indicator limiting the capacity of the system – despite the fact that these

solutions represent an upper limit on the likely capacity. For the curved girder geometry, the curve offsets, as denoted by "*h*" in Fig. 9, is akin to the maximum imperfection value $\Delta_0$ of the straight girders, which will likely translate to very large values with greater girder curvature (smaller *R*).

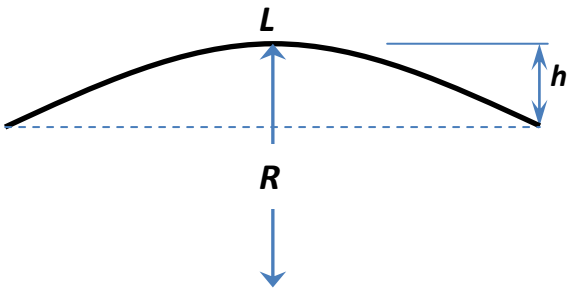


Figure 9. Schematic Diagram of Curved Geometry

To investigate the non-linear displacement behavior of curved girder system, three load-deflection analyses labeled R1 to R3 were performed on curved two-span continuous twin I-girder systems as depicted in Fig. 10. The girder systems for all three analyses were equally spanned by 140 ft. and spaced at 7 ft. with radius of curvature R varying from 1000 ft., 2000 ft., and 3000 ft., resulting in respective curve offsets of 29.4 in., 14.7 in., and 9.8 in. and respective *L*/*R* ratios 0.14, 0.07, and 0.047. Girders were assumed perfectly curved with no initial imperfection assigned.

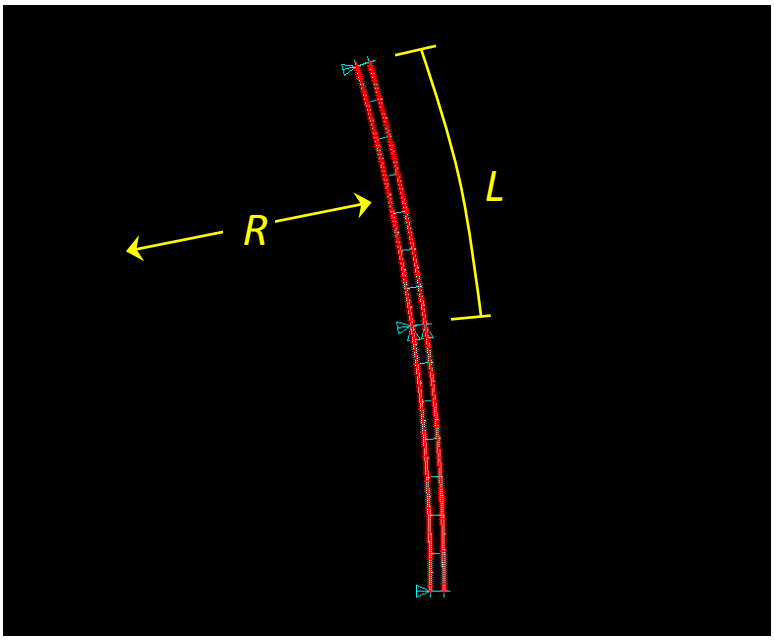


Figure 10. FE Model of Curved Two Span Twin I-Girder System

Fig. 11 contains a graph showing the graphs of load versus lateral displacement which is examined at mid-span for all three analyses. The loads are normalized by their elastic buckling loads while the lateral displacements are normalized by the value $\Delta_0 = L/1000 = 1.68$ in. for the sake of comparison with previous analyses though no imperfection is assign for curved systems. It is evident that the second-order amplification effect for lateral torsional displacement increases

with greater curvature. It should be nevertheless noticed that despite the fact that the horizontally-curved girder geometries have considerable "imperfection-like" curve offsets, the magnitude of the lateral displacements are not proportional to the offset. At 70% of the elastic buckling loads, the normalized lateral displacements are 2.61 (4.38 in.), 1.38 (2.31 in.), 0.93 (1.56 in.), respectively for curve offset values of 29.4 in., 14.7 in., and 9.8 in. Further analyses of this study are ongoing. The authors are examining the curved systems with greater radius of curvature. The goal of the parametric studies on horizontally curved girders is to identify a degree of curvature that can be used so that 70% of the critical load provided by Eq. (1) can be used as a limit. For more curved systems, the specification would require a second order analysis to fully understand the behavior.

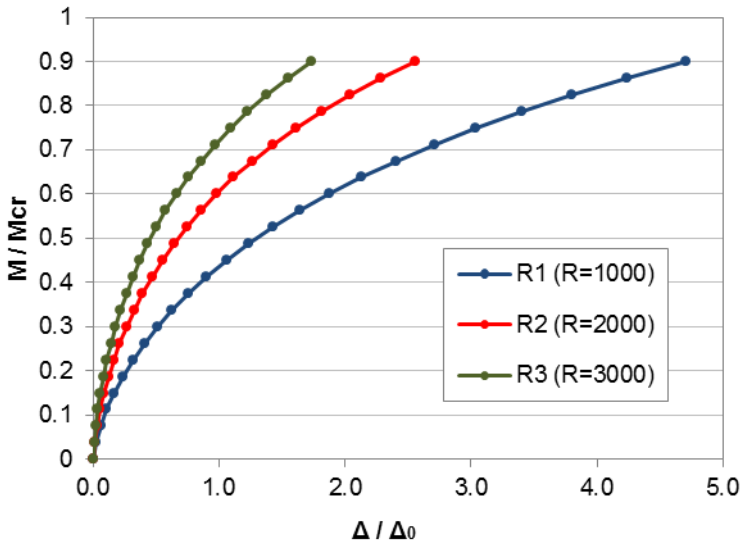


Figure 11. Normalized Load vs Displacement Curves for Curved Systems

## 6. Conclusions

An earlier study (Han and Helwig 2016) on non-linear buckling behavior of a simply-supported twin I-girder system reveals that "twist-dominant" cross-sectional shape is the most critical to the second-order amplification of lateral-torsional displacement. In spite of this, the simulation of cross frame installation process conducted in this study shows that the fit-up of cross frames would alter the initial cross-sectional shape of imperfection. After the installation, the two girders will have the same cross-sectional shape which is close to "pure sweep" type regardless of the initial cross-sectional shapes of two girders, therefore significantly reducing the possible second–order displacement amplification.

For continuous girder systems which have two or more spans, the study shows that the distribution of imperfection has a profound effect on their non-linear buckling behavior. The most critical distribution of imperfection would have a zigzagging pattern in which the lateral directions of girder imperfections alternate in the neighboring spans. The findings of this study along with previous research provide insight into the development of proper limits on second-order displacement amplification of I-girder systems as a function of the geometry of the system.

For curved girder systems, despite their geometric resemblance to straight girders with wave imperfection distributions of significant magnitude. The lateral displacement amplifications for them are not proportional to the imperfection-like arch height of the horizontally-curved girder geometry. Nevertheless, the second-order displacement amplification increases with greater span curvature. The load-deflection analyses indicate that for slightly-curved (($L/R$<0.05) systems, the girders can be loaded up to 70% of elastic buckling capacities without causing excessive second-order displacement amplification. For girder systems with greater curvature, further nonlinear load-deflection analysis is necessary.

## Notation

The following symbols are used in this paper:

$C_{bs}$ = moment gradient for system mode buckling of I-girder systems
$E$ = modulus of elasticity
$h$ = arch height of the curved girder geometry
$I_x$ = moment of inertia about the strong axis of a single girder
$I_y$ = moment of inertia about the weak axis of a single girder
$L$ = span lenghth
$M_g$ = total moment resistance of the girder system
$R$ = radius of curvature
$s$ = girder spacing

## References


AASHTO (2015), "LRFD Bridge Design Specifications", 7th Ed. Washington DC.

ANSYS (2015), Version 14.5 Academic Research, General Purpose Finite Element Software, Canonsburg, PA.

Battistini, A., Wang, W., Helwig, T., Engelhardt, M., and Frank, K.; (2016) "Stiffness Behavior of Cross Frames in Steel Bridge Systems," ASCE Journal of Bridge Engineering, 21(6 , 04016024.

Han, L, Helwig, T.A. (2016). "Effect of Girder Continuity and Imperfections on System Buckling of Narrow I-girder Systems" *Proceedings of Annual Stability Conference*, Orlando, Florida.

Helwig, T.A. (1994). "Lateral Bracing of Bridge Girders by Metal Deck Forms." *Ph.D. Dissertation Submitted to University of Texas.* Austin, TX.

Helwig, T.A., Frank, K.H., and Yura, J.A. (1997). "Lateral-Torsional Buckling of Singly Symmetric I-Beams." *Journal of Structural Engineering*, 123 (9) 1172-1179.

Quadrato, C.E. (2010). "Stability of Skewed I-shaped Girder Bridges Using Bent Plate Connections." *Ph.D. Dissertation Submitted to University of Texas.* Austin, TX.

Sanchez, T.A., White, D.W. (2012). "Stability of Curved Steel I-Girder Bridges During Construction" *Transportation Research Record: Journal of the Transportation Research Board*, (2268) 122-129.

Stith, J.C. (2010). "Predicting the Behavior of Horizontally Curved I-Girders During Construction." *Ph.D. Dissertation Submitted to University of Texas.* Austin, TX.

Wang, L. and Helwig, T.A., "Critical Imperfections for Beam Bracing Systems," *ASCE Journal of Structural Engineering*, Vol. 131, No. 6, pp. 933-940, June 2005.

Yura, J.A., Widianto, J.A. (2005). "Lateral buckling and bracing of beams—A re-evaluation after the Marcy bridge collapse." *Proceedings of Structural Stability Research Council*, Montreal. 277-294.

Yura, J.A., Helwig, T.A., Herman, R., Zhou, C. (2008). "Global Lateral Buckling of I-Shaped Girder Systems." *Journal of Structural Engineering*, 134 (9) 1487-1494.